Clays and Clay Minerals, Vol. 58, No. 3, 431–448, 2010.

APPLICATION OF BOX–BEHNKEN DESIGN TO MODELING THE EFFECT OF SMECTITE CONTENT ON SWELLING TO HYDROCYCLONE PROCESSING OF BENTONITES WITH VARIOUS GEOLOGIC PROPERTIES

SELÇUK ÖZGEN* AND AHMET YILDIZ

Department of Mining Engineering, Afyon Kocatepe University, 03200 Afyonkarahisar, Turkey

Abstract—As advances in technology have led to increased use of bentonites, more high-quality bentonite has been sought. The volume of high-quality bentonites available is shrinking and use of bentonite reserves containing impurities is inevitable. The aim of this study was to apply Box–Behnken experimental design and response surface methodology to model and optimize some operational parameters of a hydrocyclone to produce three groups of bentonite concentrates. The four significant operational parameters of hydrocyclones are feed solid ratio, inlet pressure, vortex diameter, and apex diameter, and these parameters were varied and the results evaluated using the Box–Behnken factorial design. In order to produce bentonite concentrates using a hydrocyclone, mathematical model equations were derived by computer simulation programming applying a least-squares method, using *Minitab 15*. Second-order response functions were produced for the swelling and to establish the quantity of smectite in the bentonite concentrates. Predicted values were found to be in good agreement with the experimental values (R^2 values of between 0.829 and 0.999 for smectite and three different swelling groups for the bentonites). Although in natural states these bentonites are not suitable for industrial use, enhancements were obtained giving up to 81.45% smectite and by increasing swelling by 194% for the three bentonite groups. The swelling properties of the bentonites are improved by increasing the proportion of smectite content. The graphics were designed to relate swelling and smectite content according to the two-dimensional hydrocyclone factors, and each factor was evaluated in itself. The present study revealed that the Box–Behnken and response surface methodology can be applied efficiently to model the hydrocyclone for bentonite; the method is economical and provides the maximum amount of information in a short period of time and with the smallest number of experiments.

Key Words—Bentonite, Box–Behnken Design, Clay Minerals, Hydrocyclone, Modeling, Process Optimization, Response Surface Methodology, Optimization, Smectite, Swelling.

INTRODUCTION

Bentonite is generally an impure clay consisting mostly of smectite minerals and is particularly valued due to its remarkable physical and chemical properties, which make it suitable for many industrial applications (Grim and Güven, 1978). Smectite is a family name and includes montmorillonite, beidellite, hectorite, and saponite minerals (Grim, 1968).

The commercial importance of bentonites depends on the quality and quantity of smectites and other minerals, the valence state of the exchangeable cations, the type of exchange cation, and cation exchange capacity (CEC) (Luckham and Rossi, 1999; Murray, 2000; Önal, 2007; Yıldız and Kuscu, 2007). Some physicochemical properties can change considerably as a result of acid activation, soda activation, ion exchange, and heating processes (Theng, 1974; Pinnavaia, 1983; Lagaly, 1984; Alter, 1986; Adams, 1987; Barrer, 1989; Ge *et al*., 1994; Komadel *et al*., 1996; Christidis *et al*., 1997; Christidis, 1998; Sarıkaya *et al*., 2000; Önal *et al*., 2002; Varma, 2002; Komadel, 2003; Tan *et al*., 2004; Kahraman *et al*., 2005; Önal, 2007).

The physical state of a bentonite can be changed from a dry solid to a hydrated solid, a semi-rigid plastic, a gel, and a suspension, respectively, with increasing water content (Low, 1979; Sharmm and Kwak, 1982; Güven and Pollastro, 1992; Malfoy *et al*., 2003; Önal, 2007). Bentonite-water systems are of vital importance for agricultural, industrial, environmental, and civil engineering applications such as preparation of desiccants, sealants, ceramics, cat litter, iron ore pellets, molding sand for foundry use, drilling mud for oil recovery, and subsurface barriers for water and nuclear waste (Grim and Güven, 1978; Kahr *et al*., 1990; Push, 1992; Komine and Ogata, 1999; Yong, 1999; Neaman *et al*., 2003; Wersin *et al*., 2004; Önal, 2007).

Bentonite contains not only swelling clay minerals such as montmorillonite but also non-swelling minerals such as quartz, calcite, etc. The swelling clay minerals expand by adsorbing water and filling the voids in the compacted bentonite (Komine and Ogata, 1994, 1996). The non-clay minerals in bentonite have a negative effect on the swelling properties (Christidis and Scott, 1993; Allo and Murray, 2004; Yıldız and Kuscu, 2007).

* E-mail address of corresponding author:
sozgen@aku.edu.tr
DOI: 10.1346/CCMN.2010.0580312

Most studies on the swelling of bentonites have focused on the increase in basal spacing which depends on the bentonite mineralogy, the degree to which water is taken up, and also size, valence, electronegativity, and hydration energy of the exchangeable cations. As higher-quality bentonite reserves have diminished the use of lower-grade materials has become necessary. Enrichment of bentonites is very important in the production of bentonite-based products such as bleaching earth, material for cosmetics, and for use in medicine (Boylu *et al*., 2007).

When clay systems with impurities are resettled or dispersed in water, they reveal two different size groups. Impurities and clays form clusters of different sizes when submerged and kept in water for a certain amount of time. Different clay minerals have similar particle densities but can be separated according to their particle size (Boylu *et al*., 2007). Non-clay mineral impurities in bentonite, such as quartz, calcite, etc., can also be removed through beneficiation processes to separate the smectite (Hassan and Abdel-Khalek 1998).

Although enrichment of bentonites is relatively easy, costs are a consideration. Small solid:liquid ratios are adopted in some wet-processing methods, such as the hydrocyclone. Because viscosity is a function of the solids rate, the increase in viscosity that results from mixing bentonite with water limits the ability of the hydrocyclone to remove non-clay particles by increasing the centrifugal force required to achieve separation. The hydrocyclone does, however, still have advantages over beneficiation by decantation in the enhancement of bentonites.

Mineral processes use hydrocyclone separators to perform separations on the basis of size and/or density differences between the dispersed particulate phases (Williams *et al*., 1994; Rickwood *et al.*, 1992). A hydrocyclone consists of two main parts (Figure 1). The first is a cylindrical part, with an inlet through which the feed enters tangentially. This part also includes an outlet, located at the top of the cylinder, extends into the cylinder and is known as the vortex finder. The second main part is conical and is connected to the cylindrical section at the top and to the underflow at the bottom end. The latter part is known as the spigot. The centrifugation forces exerted by the vortex cause larger particles to migrate to the cyclone wall where they are discharged through the underflow orifice. Small particles move to the central axis of the cyclone and are carried out by the overflow stream (Habibian *et al.*, 2008). The parameters that affect the performance of the hydrocyclone are the feed solid ratio (%), inlet pressure (bar), vortex diameter (mm), apex diameter (mm), viscosity of the feed stock (cP), and cyclone diameter (mm). The success of the hydrocyclone depends on the selection of suitable parameter levels and minerals. Optimization of the parameters requires many tests.

The total number of experiments required can be reduced by careful choice of the experimental design technique (Özbayoğlu and Atalay, 2000; Aslan, 2007a).

Experimental design is a systematic, rigorous approach to engineering problem solving that applies principles and techniques at the data-collection stage so as to ensure the generation of valid, precise, and accurate engineering conclusions (Xiao and Vien, 2004; Aslan, 2007b; Özgen *et al.*, 2009). Experimental design is a very economical means of extracting the maximum amount of complex information, while saving significant experimental time and material (Kincl *et al.*, 2005; Aslan, 2007b; Özgen *et al.*, 2009). Furthermore, analysis of the results is easy and experimental errors are minimized. A statistical method measures the effects of change in the operating variables and their combined interactions on the processes (Box *et al.*, 1978).

The design of experiments leads to unique response surface methodologies using mathematical and statistical techniques, with important applications not only for new products but also in the improvement of the design of existing products. With this aim in mind, one must first select the appropriate mixtures from which the response surface might be calculated; then the property value can be predicted for any design, depending on changes in the proportions of its components (Box and Behnken, 1960; Ragonese *et al.*, 2002, Correia *et al.*, 2004; Aslan, 2007b; Özgen *et al.*, 2009).

Experimental design methods and response surface methodologies are used widely for modeling process parameters, especially in chemical processes and pharmaceutical systems. To date, experimental design has not, however, been applied widely to mineral-processing systems. The central composite design here has been used successfully to design an experimental program to provide data to model the effects of inlet pressure, feed

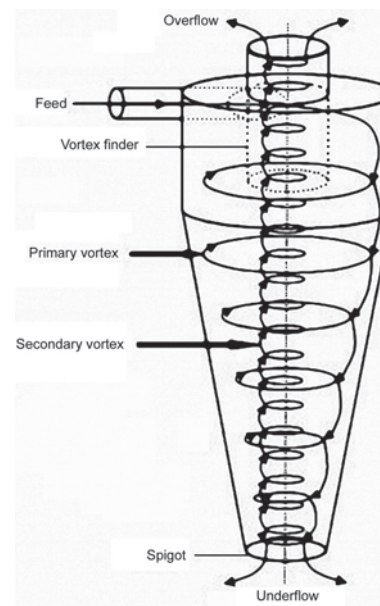

Figure 1. Schematic diagram of a hydrocyclone.

density, and length and diameter of the inner vortex finder on the operational performance of a 150 mm three-product cyclone (Obeng *et al.*, 2005). The Box–Wilson statistical experimental design method was employed to evaluate the effects of important variables such as bridging liquid (oil) concentration, salt ($CaCl_2.2H_2O$) concentration, and stirring speed on the agglomeration of bituminous coal (Cebeci and Sönmez, 2006). The response surface methodology and Box−Behnken design have been discussed for possible modeling of bond-work indexes for some Turkish coals by Aslan and Cebeci (2007). A study of flotation tests of synthetic mixtures of celestite ($SrSO_4$) and calcite ($CaCO_3$) minerals using a factorial experimental design was carried out by Martinez *et al.* (2003). Aslan (2007a) discussed the application of response surface methodology and central composite rotatable design for modeling the influence of some operating variables on the performance of a Multi-Gravity Separator (Mozley, Gloucester, UK) for coal cleaning. Finally, Aslan (2007b) developed a three-level Box–Behnken factorial design combined with response surface methodology for modeling and optimizing some operations parameters of a Multi Gravity Separator to produce a celestite concentrate.

Except for Aslan (2007b), all of the aforementioned studies involve experiment design and/or modeling, but not optimization. In mineral-processing operations, comparative trials are sometimes essential in order to determine which operating conditions achieve better performance. Usually, this is the case for a new concentrator or circuit design. In some mineral-concentration plants a 1% or 2% improvement in recovery and/or grade may be economically remarkable. Both modeling and optimization to reach maximum grade and/or recovery are very important issues in these processes (Aslan, 2007b).

In the present study, the smectite content and the swelling properties of the bentonites extracted from three separate regions previously deemed unsuitable for industrial use (due to their small smectite content and poor swelling volume) were enhanced through beneficiation. Hydrocyclones have played a very significant role in bentonite concentration. The optimization of four operational variables of a hydrocyclone (feed solid ratio, inlet pressure, vortex diameter, apex diameter) was, therefore, the aim in the present study. The use of Box–Behnken design and response surface methodology, already successfully applied in other fields, is well suited to the study of the main and interaction effects of the variables in bentonite concentration using the hydrocyclone.

Below, the requirements for the Box−Behnken design with response surface method and their applications to the design of experiments and modeling of the hydrocyclone are described. Optimization of these operational variables for maximum swelling and the greatest proportion of smectite in the bentonite concentrate was achieved using quadratic programming of the mathematical software package *Minitab 15* (Minitab Inc., 2007).

MATERIALS AND METHODS

Bentonite samples were collected from various stratigraphic levels of the bentonite deposits between the Mihalgazi and Sarıcakaya districts in Eskişehir (Western Turkey) (Figure 2). Bentonite deposits in this region were formed by alteration of andesitic and dacitic volcanic rocks. The bentonites are classified in three groups based on their geologic features; bentonite deposits in andesitic and dacitic lavas, bentonite deposits in andesitic agglomerate, and bentonite deposits in tuff (Yıldız *et al.*, 2008).

Figure 2. Location map.

Table 1. Sample properties from the experimental study.

Properties		Bentonites		
		Group 1	Group 2	Group 3
Particle size (wet), μm		−500	−500	−500
Cation exchange capacity, meq/100 g		32.6	57.1	43.5
Swelling, mL/2 g		6	10	8
Viscosity, cP FANN (600 rpm)	5% solids	4.5	5.5	4.5
	7.5% solids	5.5	6.5	5.5
	10% solids	6.5	8	6.5

Characterization test results of the three samples are given in Table 1. Here, the CEC values of each bentonite group were determined by the methylene blue (MB) standard method (Rytwo *et al*., 1991; Önal, 2007) and viscosity values were measured with 5, 7.5, or 10% solids at 600 rpm using a Fann viscosimeter at Turkish General Directorate of Mineral Research & Exploration. The swelling of each sample was measured as the total volume of a gel formed from a 2 g sample in 100 mL of water (ASTM D 5890-95). The CEC, viscosity, and swelling volume of the raw bentonites were relatively small (Table 1). The second group of bentonites had the best physical properties. Chemical analyses of major oxides were obtained by inductively coupled plasma-mass spectrometry (ICP-MS) at the ACME analytical laboratory, Canada (Table 2), and chemical analyses revealed that the $CaO+Na_2O$ totals of all three bentonites were in the range 4.28−7.00%. Mineralogical investigations were carried out on processed and random powder samples by means of X-ray diffraction (XRD) analysis, using a Rigaku Geiger Flex Diffractometer with Ni-filtered CuKα radiation. The scanning speed for all samples was 2°2θ/min. Smectite and the other mineral contents of the samples were determined by semi-quantitative interpretation of the XRD data (without standards). The reflections, peak intensity, and Reference Intensity Ratio (RIR) of minerals were analyzed by the formulae of Chung (1974), which enabled calculation of mineral abundances as weight percentages. This method was chosen because it yields reproducible results and has been used by other researchers (Biscaye, 1965; Johns *et al.*, 1954; Gündoğdu, 1982), thus giving the mineral contents of the present samples. Morphological and mineralogical studies were carried out using a LEO VP-1431 (Korea) scanning electron microscope (SEM) with EDS equipment. The XRD patterns indicated that smectite was the major mineral phase in the bulk samples (Table 3; Figure 3) (Grim, 1962; Brown and Brindley, 1980; Brown, 1972). Illite and chlorite were minor constituents. Non-clay minerals in the samples included cristobalite/opal-CT, quartz, feldspar, calcite, and dolomite. The smectite content, which affects the performance of the bentonites in various industrial applications, was 54%, 55%, and 40% in Groups 1, 2, and 3, respectively. Feldspar was a major impurity in all groups and the amount of feldspar was 40%, 32%, and 30% in Groups 1, 2, and 3, respectively. The cristobalite/opal-CT contents of the bentonites in Groups 1, 2, and 3 were 0 wt.%, 5 wt.%, and 7 wt.%, respectively (Table 3). Cristobalite/opal-CT minerals are somewhat similar to smectites with respect to their physical properties such as density, crystal size, etc. The XRD investigations revealed that the bentonites in Groups 1 and 2 consisted

Table 2. Chemical composition (wt.%) of the bentonites used in the experiments.

Component	Content (%)		
	Group 1	Group 2	Group 3
Na_2O	2.80	1.35	1.90
MgO	1.69	3.84	6.22
Al_2O_3	22.74	16.19	13.73
SiO_2	54.01	52.81	51.40
P_2O_5	0.14	0.16	0.15
K_2O	0.23	1.69	1.70
CaO	3.97	2.93	5.10
MnO	0.02	0.08	0.09
TiO_2	0.79	0.84	0.81
Fe_2O_3	3.66	6.28	6.03
LOI	9.90	14.00	13.00
Total	99.95	100.07	99.93

LOI: loss on ignition

Table 3. Mineralogical analysis (wt.%) of the bentonites used in the experiments.

Minerals	Content (%)		
	Group 1	Group 2	Group 3
Smectite	54.0	55.0	40.0
Illite	1.0	0.0	2.0
Chlorite	12.0	0.0	0.0
Cristobalite/Opal CT	0.0	5.0	7.0
Quartz	2.0	2.0	4.0
Feldspar	40.0	32.0	30.0
Calcite	2.0	3.0	9.0
Dolomite	0.0	3.0	8.0
Total	99.0	100.0	100.0

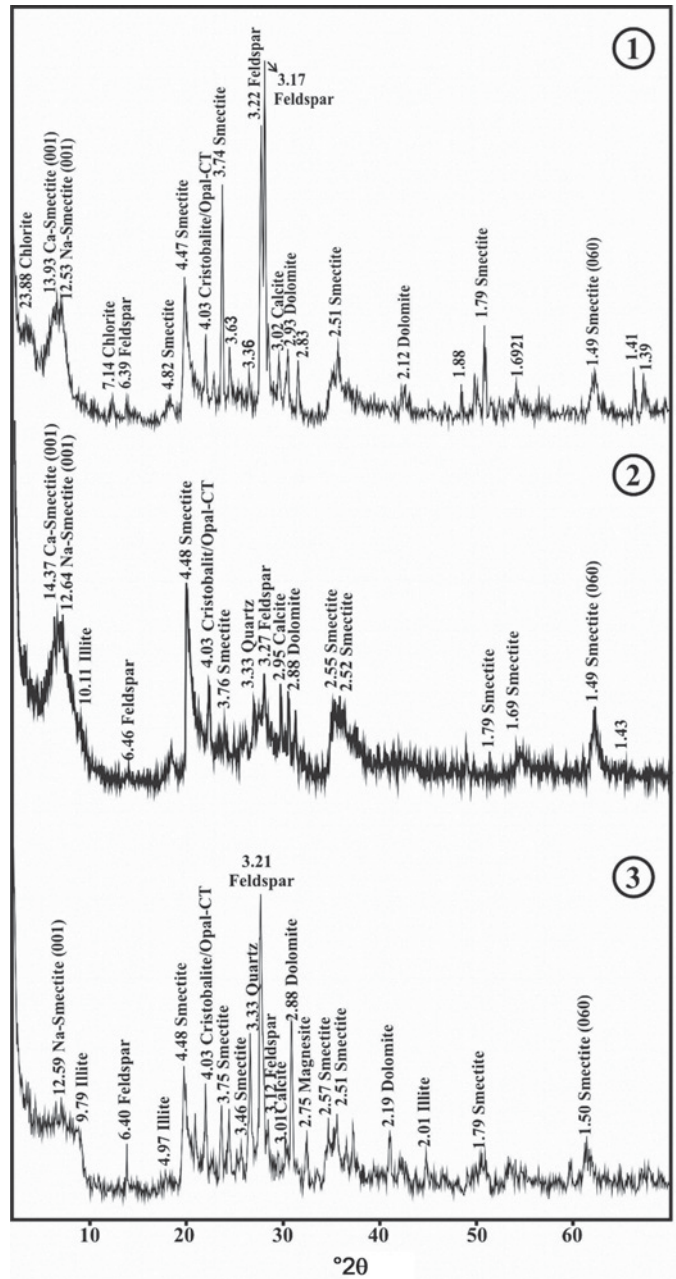

Figure 3. XRD patterns of the bentonite used in the experiments.

of mixed (Na-Ca) smectites; Group 3 included Na-smectites. The Na_2O contents of bentonites were determined as 1.52 wt.% (Group 1), 3.24 wt.% (Group 2), and 2.52 wt.% (Group 3) in EDS studies (Figure 4). The XRD and EDS studies show that the Na^+ is the primary exchangeable cation in smectites of Groups 2 and 3. The swelling properties of the Na-smectite are commonly more developed than those of Ca-smectite (Luckham and Rossi, 1999).

The Box–Behnken design (Box *et al.*, 1978; Box and Wilson, 1951; Box and Behnken, 1960; Montgomery, 2001; Ferreira *et al.*, 2004; Souza Anderson *et al.*, 2005; Aslan and Cebeci, 2007) is a rotatable second-order design based on three-level incomplete factorial designs. The special arrangement of the Box–Behnken design levels allows the number of design points to increase at the same rate as the number of polynomial coefficients. For three factors, for example, the design can be constructed as three blocks of four experiments consisting of a full two-factor factorial design with the level of the third factor set at zero (Souza Anderson *et al.*, 2005; Aslan and Cebeci, 2007).

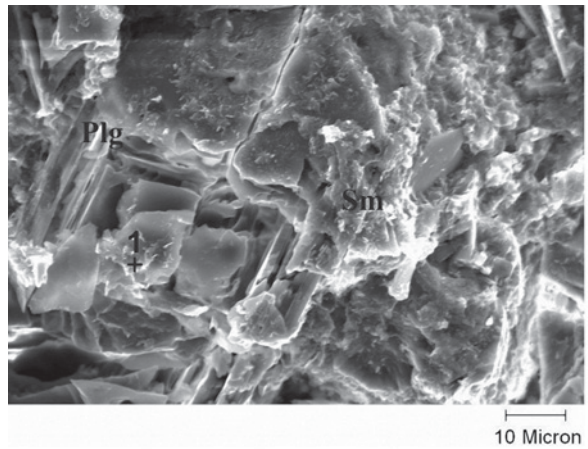

Group 1

Oxides (%)	Spectrum 1
Na_2O	1.52
MgO	0.58
Al_2O_3	23.15
SiO_2	62.82
CaO	9.42
Fe_2O_3	2.52
Total	100.01

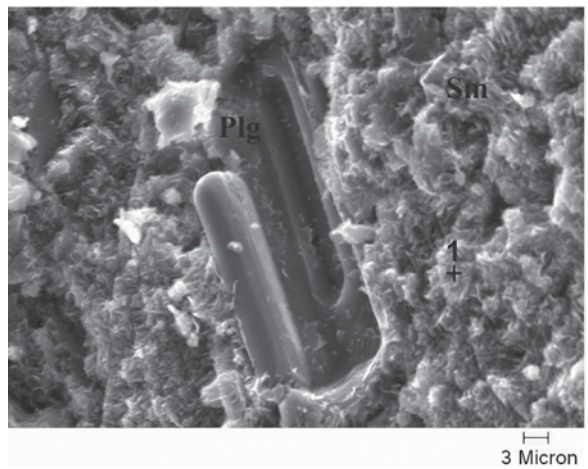

Group 2

Oxides (%)	Spectrum 1
Na_2O	3.24
MgO	3.76
Al_2O_3	20.72
SiO_2	62.12
K_2O	0.74
CaO	0.90
Fe_2O_3	8.52
Total	100.00

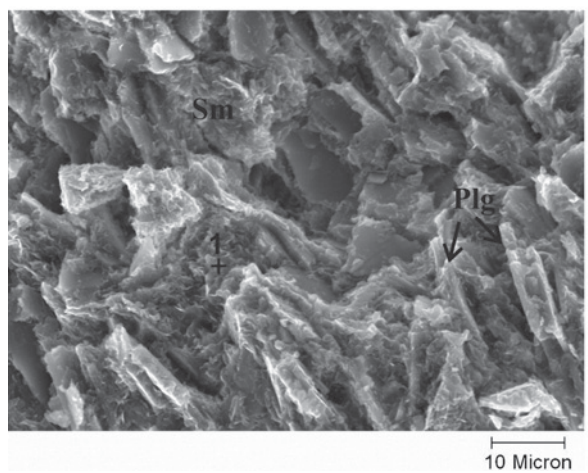

Group 2

Oxides (%)	Spectrum 1
Na_2O	2.52
MgO	4.15
Al_2O_3	18.29
SiO_2	66.86
K_2O	1.91
CaO	0.30
Fe_2O_3	5.97
Total	100.00

Figure 4. EDS analyses of the bentonite used in the experiments.

In the present study, the Box–Behnken factorial design was chosen to discover the relationship between the response functions (smectite concentration and swelling of the bentonite concentrate) and four variables of the hydrocyclone (feed solid, inlet pressure, vortex diameter, and apex diameter), while holding other operational parameters of the hydrocyclone constant (cyclone diameter of 44 mm, feed suspension of 30 L,

pre-feed mixture in mixer for 5 min). Batch hydrocyclone tests were conducted at the mineral processing laboratory of Afyon Kocatepe University, Turkey.

Samples were dried at 60°C and then added to water (10% solids); the suspension was settled for 24 h and stirred for 2−3 h by a propeller agitator. The suspension was passed through a 500 μm sieve and then fed into the hydrocyclone. The solid:liquid ratio was regulated by addition of water. The suspension was stirred using a centrifugal pump (with by-pass valve) for 5 min to achieve homogeneity (in the system). Later, material was fed into the hydrocyclone by closing the by-pass valve, and two discrete overflow and underflow products were obtained. The samples were filtered, dried, and analyzed for smectite content and swelling (Figure 5).

Response surface methodology (RSM)

Response surface methodology is a collection of statistical and mathematical methods that are useful for modeling and analyzing engineering problems. The main objective is to optimize the response surface that is influenced by various process parameters. Response surface methodology also quantifies the relationship between the controllable input parameters and the response surfaces obtained (Kwak, 2005; Aslan and Cebeci, 2007; Aslan, 2007a, 2007b).

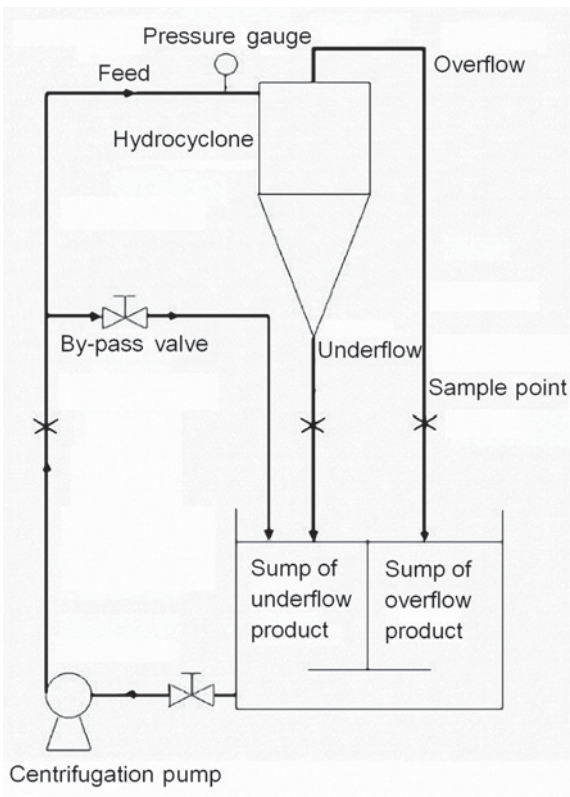

Figure 5. Hydrocyclone experimental setup.

The design of the response surface methodology consisted of the following (Gunaraj and Murugan, 1999; Kwak, 2005; Aslan and Cebeci, 2007; Aslan, 2007a, 2007b): (1) designing a series of experiments for adequate and reliable measurement of the response of interest; (2) developing a mathematical model of the second-order response surface with the best fittings; (3) finding the optimal set of experimental parameters to produce a maximum or minimum value of response; and (4) representing the direct and interactive effects of process parameters through two-dimensional (3D) and three-dimensional (3D) plots.

If all variables are assumed to be measurable, the response surface can be expressed as follows (equation 1):

$$y = f(x_1, x_2, x_3, \ldots, x_k) \quad (1)$$

where y is the response variable, and $x_i = x_1, x_2, x_3$, or x_k are the controlling variables referred to as factors.

The goal of this aspect of the study was to optimize the response variable y. The independent variables are assumed to be continuous and controllable by the experiments with negligible errors. A reasonable approximation for the true functional relationship between independent variables and the response surface is desired. A second-order model is usually used in response surface methodology (Gunaraj and Murugan, 1999; Kwak, 2005; Aslan and Cebeci, 2007; Aslan, 2007a, 2007b):

$$y = \beta_0 + \sum_{i=1}^{k} \beta_i x_i + \sum_{i=1}^{k} \beta_{ii} x_i^2 + \sum_{i=1}^{k-1} \sum_{j=2}^{k} \beta_{ij} x_i x_j + \varepsilon \quad (2)$$

where $x_1, x_2, \ldots, x_k$ are the input factors which influence the response y; β_0, β_{ii} ($i = 1, 2, \ldots, k$), β_{ij} ($i = 1,2,\ldots,k$; $j = 1,2,\ldots,k$) are unknown parameters, and ε is a random error term. The β coefficients, which should be determined in the second-order model, are obtained by the least-squares method. In general equation 2 can be written in matrix form (Kincl *et al.*, 2005; Kwak, 2005; Aslan and Cebeci, 2007; Aslan, 2007a, 2007b):

$$Y = bX + \varepsilon \quad (3)$$

where Y is a matrix of measured values and X is a matrix of independent variables. The matrices b and ε consist of coefficients and errors, respectively. The solution of equation 3 can be obtained by the matrix approach (Gunaraj and Murugan, 1999; Kwak, 2005; Aslan and Cebeci, 2007; Aslan, 2007a, 2007b).

$$b = (X^T X)^{-1} X^T Y \quad (4)$$

where X^T is the transpose of the matrix X and $(X^T X)^{-1}$ is the inverse of the matrix $X^T X$ (Kwak, 2005; Aslan and Cebeci, 2007; Aslan, 2007a, 2007b).

The coefficients, *i.e.* the main effect (b_i) and the two-factor interactions (b_{ij}), can be estimated from the experimental results by computer-simulation programming applying the least-squares method using *Minitab 15* (Minitab Inc., 2007).

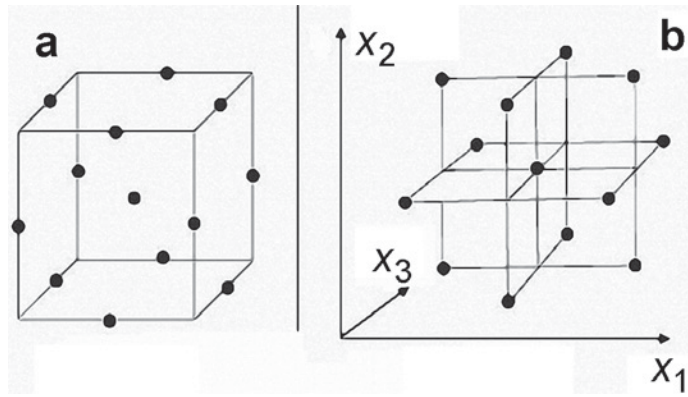

Figure 6. Box-Behnken design. (a) The design, as derived from a cube; (b) representation as interlocking 2^2 factorial experiments.

Experimental design for the hydrocyclone tests

Box–Behnken design requires an experiment number according to $N = k^2 + k + c_p$, where k is the factor number and c_p is the replicate number of the mid-point (Massart *et al.*, 1997; Neto *et al.*, 2001; Ferreira *et al.*, 2004; Souza Anderson *et al.*, 2005; Aslan, 2007b;). Box–Behnken is a spherical, revolving design. Viewed as a cube (Figure 6a) (Souza Anderson *et al.*, 2005; Massart *et al.*, 1997; Aslan and Cebeci, 2007), the Box–Behnken design consists of a central point and the middle points of the edges. However, it can also be viewed as consisting of three interlocking 2^2 factorial designs and a central point (Figure 6b) (Souza Anderson *et al.*, 2005; Massart *et al.*, 1997; Aslan and Cebeci, 2007).

For the three-level, four-factorial Box–Behnken experimental design, 27 experimental runs in total ($\binom{4}{2}4 + 3$ centerpoints), were needed (Table 4).

Considering the effects of the main factors and also the interactions between two-factor sets, equation 2 takes the form:

$$y = \beta_0 + \beta_1 x_1 + \beta_2 x_2 + \beta_3 x_3 + \beta_4 x_4 + \beta_{11} x_1^2 + \beta_{22} x_2^2 + \beta_{33} x_3^2 + \beta_{44} x_4^2 + \beta_{12} x_1 x_2 + \beta_{13} x_1 x_3 + \beta_{14} x_1 x_4 + \beta_{23} x_2 x_3 + \beta_{24} x_2 x_4 + \beta_{34} x_3 x_4 \quad (5)$$

where y is the predicted response, β_0 is a model constant; x_1, x_2, x_3, and x_4 are independent variables; β_1, β_2, β_3, and β_4 are linear coefficients; β_{12}, β_{13}, β_{14}, β_{23}, β_{24}, and β_{34} are cross-product coefficients; and β_{11}, β_{22}, β_{33}, and β_{44} are the quadratic coefficients (Gunaraj and Murugan, 1999; Montgomery, 2001; Kwak, 2005; Aslan, 2007a, b; Aslan and Cebeci, 2007).

The coefficients, *i.e.* the main effect (β_i) and the two-factor interactions (β_{ij}), were estimated from the experimental results by computer-simulation programming applying the least square method using *Minitab 15* (Minitab Inc., 2007).

RESULTS AND DISCUSSION

Solid rate, inlet pressure, vortex diameter, and apex diameter were independent variables studied to predict the response. The coded/actual levels of the independent variables for each of the experiments in the design matrix were calculated (Table 5).

After processing the bentonites, an enhanced proportion of smectite/reduced amount of non-clay minerals was recorded. While the proportion of smectite improved to average values of 82.51%, 90.87%, and 60.87% in Groups 1, 2, and 3, respectively, the amount of feldspar decreased to 3%, 7%, and 13% in Groups 1, 2, and 3, respectively (Tables 6–8).

From the experimental results (Tables 6, 7, and 8), the second-order response functions representing smec-

Table 4. Four independent variables of hydrocyclone and their levels for Box–Behnken Design.

Variable	Symbol	— Coded variable level — Low −1	Center 0	High +1
Feed solids (*s*), %	x_1	5	7.5	10
Inlet pressure (*p*), bar	x_2	1.5	2	2.5
Vortex diameter (*v*), mm	x_3	8	11.15	14.3
Apex diameter, (*a*), mm	x_4	3.2	4.8	6.4

Table 5. Coded and actual levels of the four variables of hydrocyclone.

Run	Coded level of variables				Actual level of variables			
	x_1	x_2	x_3	x_4	s (%)	p (bar)	a (mm)	v (mm)
1	0	–1	0	–1	7.5	1.5	4.8	8.00
2	0	–1	–1	0	7.5	1.5	3.2	11.15
3	0	+1	0	+1	7.5	2.5	4.8	14.30
4	0	0	–1	–1	7.5	2.0	3.2	8.00
5	–1	+1	0	0	5.0	2.5	4.8	11.15
6	–1	–1	0	0	5.0	1.5	4.8	11.15
7	+1	0	+1	0	10.0	2.0	6.4	11.15
8	0	0	0	0	7.5	2.0	4.8	11.15
9	–1	0	0	+1	5.0	2.0	4.8	14.30
10	+1	0	–1	0	10.0	2.0	3.2	11.15
11	0	0	0	0	7.5	2.0	4.8	11.15
12	0	0	+1	–1	7.5	2.0	6.4	8.00
13	+1	–1	0	0	10.0	1.5	4.8	11.15
14	0	–1	0	+1	7.5	1.5	4.8	14.30
15	+1	+1	0	0	10.0	2.5	4.8	11.15
16	+1	0	0	–1	10.0	2.0	4.8	8.00
17	–1	0	0	–1	5.0	2.0	4.8	8.00
18	0	+1	0	–1	7.5	2.5	4.8	8.00
19	0	0	–1	+1	7.5	2.0	3.2	14.30
20	+1	0	0	+1	10.0	2.0	4.8	14.30
21	–1	0	–1	0	5.0	2.0	3.2	11.15
22	–1	0	+1	0	5.0	2.0	6.4	11.15
23	0	–1	+1	0	7.5	1.5	6.4	11.15
24	0	+1	+1	0	7.5	2.5	6.4	11.15
25	0	0	0	0	7.5	2.0	4.8	11.15
26	0	+1	–1	0	7.5	2.5	3.2	11.15
27	0	0	+1	+1	7.5	2.0	6.4	14.30

tite for Groups 1 (y_1), 2 (y_2), and 3 (y_3), and swelling for Groups 1 (y_4), 2 (y_5), and 3 (y_6) can be expressed as a function of feed solid ratio, inlet pressure, vortex diameter, and apex diameter. The relations between responses and variables were obtained for coded units (−1, 0, +1) for three different bentonites as follows.

The smectite contents (y_1, y_2, y_3) of the bentonites from Groups 1, 2, and 3 were:

$$y_1 = 82.33 + 0.75x_1 - 0.88x_2 + 0.17x_3 - 0.54x_4 + 0.17x_1^2 + 0.10x_2^2 + 0.04x_3^2 + 0.1x_4^2 + 0.13x_1x_2 + 0.13x_1x_4 \quad (6)$$

$$y_2 = 91.0 + 0.75x_1 + 0.88x_2 + 0.29x_3 - 0.08x_4 - 0.1x_1^2 + 0.04x_2^2 - 0.04x_3^2 - 0.01x_4^2 + 0.13x_1x_3 - 0.13x_1x_4 - 0.13x_2x_4 \quad (7)$$

$$y_3 = 61.0 - 4.38x_1 - 0.04x_2 - 2.04x_3 - 5.29x_4 - 0.04x_1^2 - 0.04x_2^2 - 0.04x_3^2 - 0.17x_4^2 + 0.13x_1x_2 + 0.13x_1x_3 - 0.13x_1x_4 \quad (8)$$

The response factor (smectite) at any regime in the interval of the experimental design can be calculated from equations 6, 7, and 8 for bentonites in Groups 1, 2, and 3, respectively.

Experimental results and the predicted values were obtained using model equations (equations 6-8 and Figures 7−9). As can be seen, the predicted values match the experimental values reasonably well, with R^2 of 0.968 for the smectite content of Group 1 bentonites, 0.973 for Group 2, and 0.999 for Group 3.

For swelling (y_4, y_5, and y_6) of the Group 1, 2, and 3 bentonites:

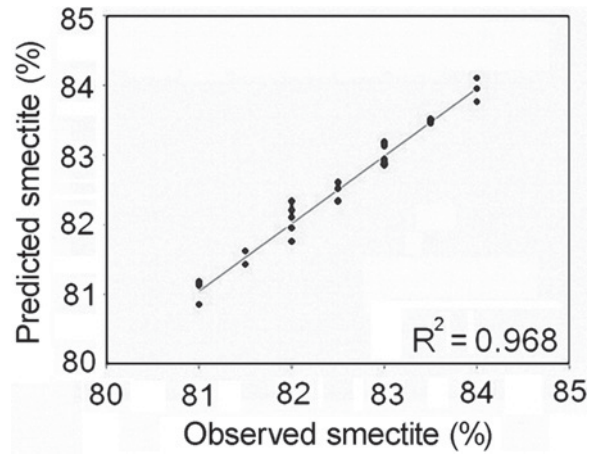

Figure 7. Relation between experimental and predicted smectite content of the Group 1 bentonites using equation 6.

Table 6. Observed and predicted values for smectite content and swelling of Group 1 bentonites.

Run	Smectite (%) Observed	Smectite (%) Predicted (R^2 = 96.80)	Recovery of smectite enrichment (%)	Swelling, (mL/2 g) Observed	Swelling, (mL/2 g) Predicted (R^2 = 82.90)
1	84.00	83.96	40.45	11.0	11.27
2	83.00	83.19	54.25	10.0	10.50
3	81.00	81.13	43.69	10.0	10.19
4	83.00	82.86	47.58	11.0	10.48
5	81.00	80.86	39.79	13.0	12.48
6	83.00	82.86	45.04	13.0	12.48
7	83.50	83.46	32.28	11.0	11.52
8	82.50	82.34	42.11	11.0	11.00
9	81.00	81.19	46.30	12.0	12.50
10	83.00	83.13	51.57	10.0	10.19
11	82.00	82.34	41.86	11.0	11.00
12	83.00	83.19	28.09	13.0	12.81
13	84.00	84.11	44.49	11.0	11.23
14	83.00	82.88	49.03	12.0	11.69
15	82.50	82.61	39.46	11.0	11.23
16	84.00	83.77	37.75	13.0	12.33
17	82.50	82.52	38.15	12.0	12.33
18	82.00	82.21	35.27	12.0	12.77
19	82.00	81.77	55.96	11.0	10.90
20	83.00	82.94	46.36	10.5	10.00
21	81.50	81.63	51.70	12.0	11.94
22	82.00	81.96	32.77	12.0	12.27
23	83.50	83.52	34.97	12.0	11.83
24	82.00	81.77	30.13	12.0	11.33
25	82.50	82.34	42.11	11.0	11.00
26	81.50	81.44	49.07	11.0	11.00
27	82.00	82.11	36.71	10.0	10.23

$$y_4 = 11.0 - 0.63x_1 - 0.42x_3 - 0.54x_4 + 0.58x_1^2 + 0.27x_2^2 - 0.10x_3^2 + 0.21x_4^2 + 0.25x_1x_3 - 0.63x_1x_4 - 0.25x_2x_3 - 0.75x_2x_4 - 0.75x_3x_4 \quad (9)$$

$$y_5 = 24.67 - 0.29x_1 + 1.25x_2 + 2.21x_3 - 0.75x_4 + 0.06x_2^2 + 0.06x_4^2 - 0.25x_1x_2 - 0.13x_1x_3 - 0.25x_1x_4 - 0.25x_2x_3 - 0.25x_2x_4 - 0.25x_3x_4 \quad (10)$$

$$y_6 = 11.00 - 1.29x_1 + 0.83x_2 - 0.71x_3 - 0.25x_4 + 2.56x_1^2 + 1.63x_2^2 + 1.31x_3^2 + 2.0x_4^2 + 0.5x_1x_2 - 0.63x_1x_3 - 0.25x_1x_4 - 0.38x_2x_3 + 0.63x_2x_4 - 0.13x_3x_4 \quad (11)$$

The response factor (swelling) from any regime in the interval of the experimental design can be calculated from equations 9, 10, and 11 for bentonites in Groups 1, 2, and 3, respectively.

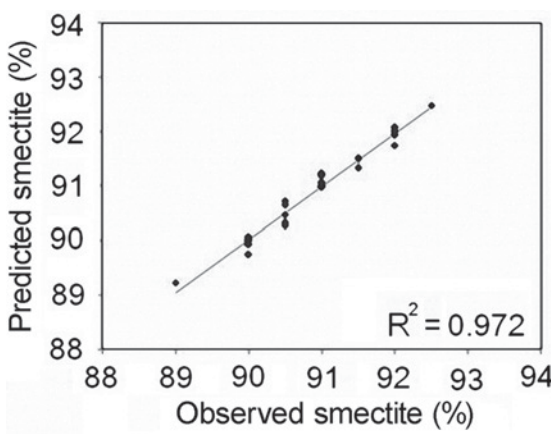

Figure 8. Relation between experimental and predicted smectite content of the Group 2 bentonites using equation 7.

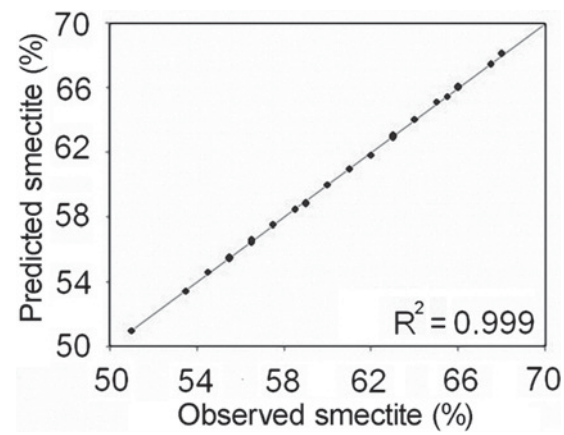

Figure 9. Relation between experimental and predicted smectite content of the Group 3 bentonites using equation 8.

Table 7. Observed and predicted values for smectite content and swelling of Group 2 bentonites.

Run	Smectite (%) Observed	Smectite (%) Predicted (R^2 = 97.29)	Recovery of smectite enrichment (%)	Swelling, (mL/2 g) Observed	Swelling, (mL/2 g) Predicted (R^2 = 99.10)
1	90.00	89.94	43.34	24.0	24.04
2	90.00	89.75	59.71	21.0	21.02
3	91.50	91.52	59.22	25.0	25.04
4	90.50	90.65	46.86	23.0	23.02
5	91.00	90.98	50.07	26.0	25.94
6	89.00	89.23	54.56	23.0	22.94
7	92.00	92.02	44.11	27.0	27.04
8	91.00	91.00	51.36	25.0	24.67
9	90.00	90.08	62.63	24.0	23.94
10	91.00	91.19	55.95	23.0	22.88
11	91.00	91.00	51.36	25.0	24.67
12	91.00	91.23	34.81	28.0	27.94
13	90.50	90.73	52.36	24.0	24.02
14	90.00	90.02	63.90	23.0	23.04
15	92.50	92.48	47.70	26.0	26.02
16	92.00	91.75	39.83	26.0	26.02
17	90.00	90.00	42.07	25.0	24.94
18	92.00	91.94	38.53	27.0	27.04
19	90.50	90.48	67.54	22.0	22.02
20	91.50	91.33	60.51	24.0	24.02
21	90.00	89.94	58.44	22.0	22.04
22	90.50	90.27	46.51	26.5	26.71
23	90.50	90.33	47.80	26.0	25.94
24	92.00	92.08	42.81	28.0	27.94
25	91.00	91.00	51.36	24.0	24.67
26	91.50	91.50	54.96	24.0	24.02
27	91.00	91.06	55.59	26.0	25.94

Experimental and predicted values (Figures 10–12) are in reasonable agreement with R^2 of 0.829 for swelling of Group 1 bentonites, 0.991 for Group 2, and 0.867 for Group 3.

Although the correlation between swelling volume and the smectite content was significant, the figures do not reflect this. The reason is that the results of the observed smectite content and swelling volume were calculated as whole numbers; multiple samples with the same result were presented and the predicted values were close to the observed values.

The effect of hydrocyclone variables on smectite and swelling. The viscosity of the feed suspension, depending on the solids rate, is the main effect on hydrocyclone performance. At greater concentrations, the suspension

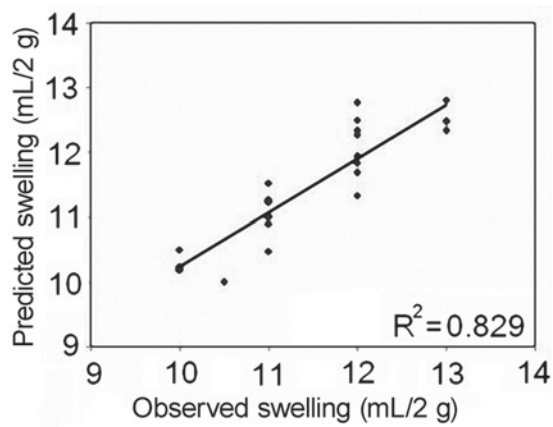

Figure 10. Relation between experimental and predicted swelling of the Group 1 bentonites using equation 9.

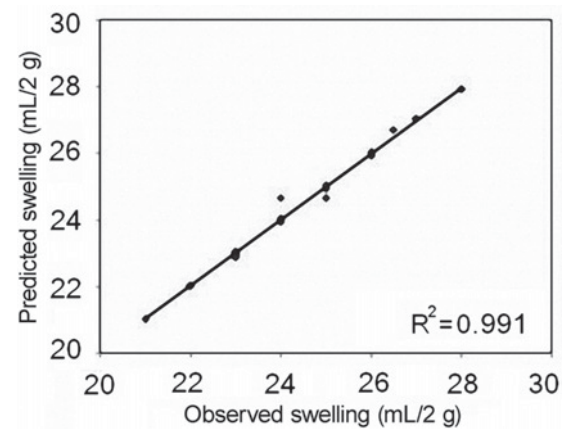

Figure 11. Relation between experimental and predicted swelling of the Group 2 bentonites using equation 10.

Table 8. Observed and predicted values for smectite content and swelling of Group 3 bentonites.

Run	Smectite (%) Observed	Smectite (%) Predicted (R^2 = 99.97)	Recovery of smectite enrichment (%)	Swelling, (mL/2 g) Observed	Swelling, (mL/2 g) Predicted (R^2 = 86.70)
1	66.00	66.12	43.27	17.0	16.33
2	63.00	63.00	67.53	14.0	15.10
3	55.50	55.46	66.09	14.0	14.17
4	68.00	68.12	58.75	15.0	15.15
5	65.00	65.12	70.73	14.0	15.15
6	65.50	65.46	67.36	17.0	17.81
7	54.50	54.62	33.23	11.0	12.25
8	61.00	61.00	56.32	11.0	11.00
9	60.00	60.00	77.76	16.0	16.35
10	58.50	58.46	56.55	14.5	14.92
11	61.00	61.00	56.32	11.0	11.00
12	64.00	64.04	32.45	14.0	13.98
13	56.50	56.46	42.85	15.0	14.23
14	55.50	55.54	62.78	15.5	14.58
15	56.50	56.62	46.22	14.0	13.56
16	62.00	61.83	34.13	14.5	14.27
17	70.50	70.33	57.85	17.0	17.35
18	66.00	66.04	47.22	13.0	13.42
19	57.50	57.54	77.02	14.5	14.90
20	51.00	51.00	52.32	14.5	14.27
21	67.50	67.46	83.48	18.0	16.25
22	63.00	63.12	55.43	17.0	16.08
23	59.00	58.92	42.18	14.0	14.44
24	59.00	58.83	45.71	13.0	12.02
25	61.00	61.00	56.32	11.0	11.00
26	63.00	62.92	71.29	14.5	14.19
27	53.50	53.46	52.56	13.0	13.23

was more viscous, so the suspension flow rate was reduced. Both the overflow and underflow flow rates were reduced, however. The centrifugal force decreased and the separation became difficult with reducing flow velocity. In order to gain a better understanding of the results, the solids rate dependencies of the smectite and swelling were depicted (Figures 13–15) (for Groups 1, 2, and 3, respectively) at a mid-level of the other three variables. When the solids rate was increased, the smectite content of the Group 2 and Group 3 bentonites decreased. The smectite content varied proportionally in Group 1 bentonites, however. Because Group 1 bentonites consisted mainly of smectite and feldspar, the processing was easy due to the different densities of the

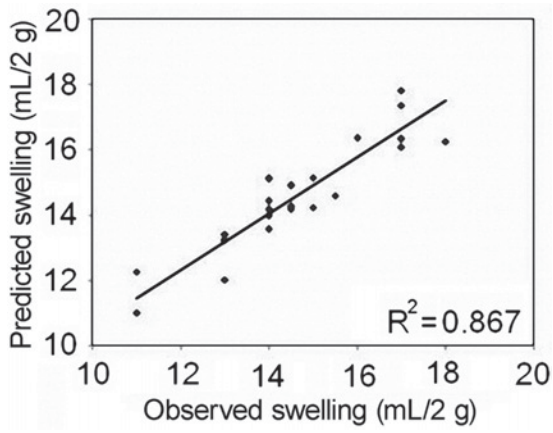

Figure 12. Relation between experimental and predicted swelling of the Group 3 bentonites using equation 11.

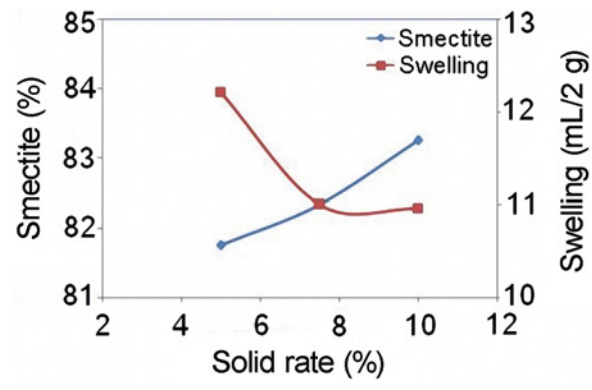

Figure 13. Variations of the smectite and swelling with different solids rate for Group 1 bentonites at the mid-level of the other three variables.

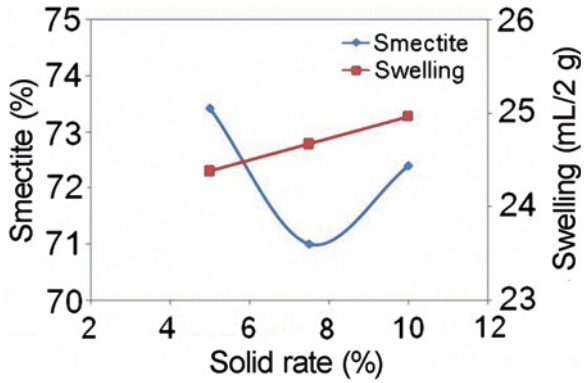

Figure 14. Variations of the smectite and swelling with different solids rate for Group 2 bentonites at the mid-level of the other three variables.

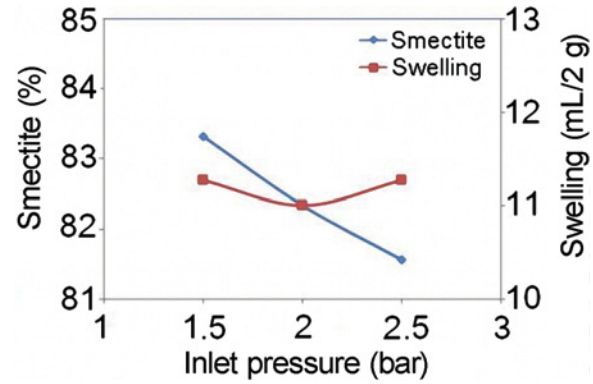

Figure 16. Variations of the smectite and swelling with different inlet pressures for Group 1 bentonites at the mid-level of the other three variables.

smectite (2.29 g/cm^3) and feldspar (2.65 g/cm^3). Group 2 and 3 bentonites included cristobalite/opal-CT along with smectite. As the density of cristobalite/opal-CT ($d_{cristobolite}$: 2.27 g/cm^3, d_{opal}: 2.10 g/cm^3) is close to that of smectite, the presence of cristobalite/opal-CT had a negative effect on the quality of the concentrate. As the solids rate increased, the viscosity increased and separation of the minerals of similar densities became more difficult. A large solids rate means that separating cristobalite/opal-CT from smectite is difficult. The abundance of silica polymorphs (cristobalite, opal-CT, and quartz), the smectite content and the nature of the interlayer cations also have an effect on the swelling volumes of bentonites (Alther, 1986; Christidis, 1998; Montes *et al.*, 2003; Yıldız and Kuşcu, 2007).

The inlet-pressure dependencies of the smectite and swelling were depicted (for Groups 1, 2, and 3, respectively) at the mid-level of the other three variables (Figures 16–18). Incremental increases of inlet pressure had a positive effect on the proportion of smectite in the bentonites of Groups 2 and 3 because the centrifugal force increased and separation of the minerals was easier with increasing inlet pressure. The smectite content and the swelling properties of Group 1 bentonites decreased, however, based on incremental increases in inlet pressure. In the Group 1 bentonites, the maximum smectite content was acquired at the smallest inlet pressure.

When the smectite contents and swelling properties were analyzed together, the smectite contents in Group 2 bentonites, which increased as a result of beneficiation, mean that swelling volume increased also. The same was observed for Group 1 bentonites at 1.5–2 bars, though the smectite contents and swelling properties decreased after 2 bars. For Group 3 bentonites, swelling decreased at pressures between 1.5 and 2 bars because swelling properties are minimal for bentonites of Groups 1 and 3 at pressures of 2 bar. The manual method of measuring the swelling volume means that the sensitivity decreases due to cumulative experimental errors as the experiment proceeds.

The variations in smectite content and swelling volume depend on the apex diameter (Figures 19–21) and the vortex diameter (Figures 22–24) (for Groups 1,

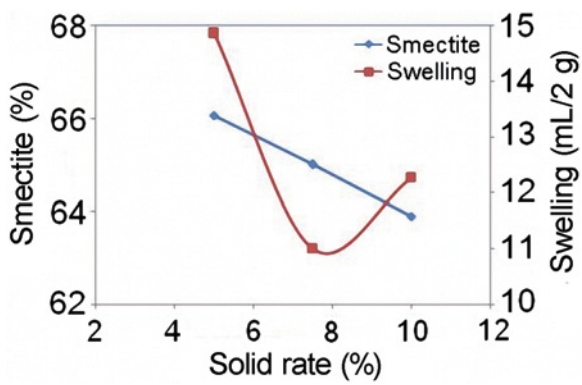

Figure 15. Variations of the smectite content and swelling with different solids rate for Group 3 bentonites at the mid-level of the other three variables.

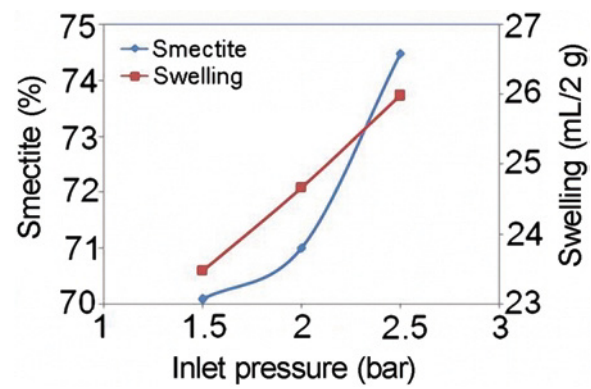

Figure 17. Variations of the smectite content and swelling with different inlet pressures for Group 2 bentonites at the mid-level of the other three variables.

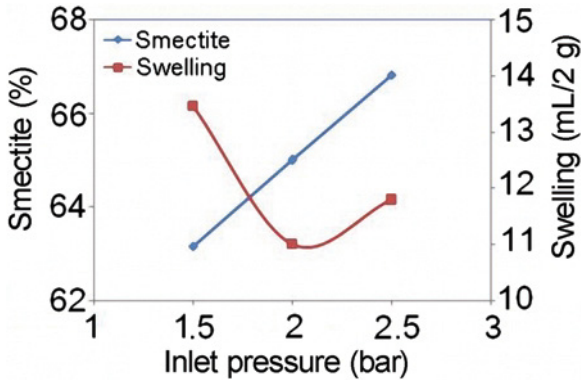

Figure 18. Variations of the smectite content and swelling with different inlet pressures for Group 3 bentonites at the mid-level of the other three variables.

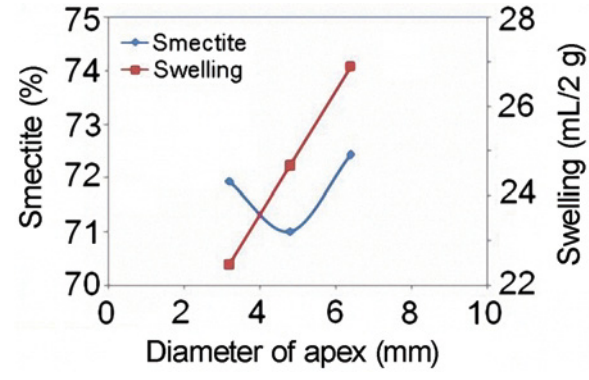

Figure 20. Variations of the smectite content and swelling with different vortex diameters for Group 2 bentonites at the mid-level of the other three variables.

2, and 3, respectively) (at mid-levels of the other three variables). While the heavy and coarse particles were obtained from the underflow (apex), the fine-grained and light particles such as clay minerals, were acquired from the overflow (vortex). The solid:liquid ratio of the suspension decreased as the diameter of the apex was increased. Therefore, the flow rate and viscosity of suspension increased also. As the centrifugal force was increased, separations of minerals of the same density were facilitated by decreasing the viscosity. When apex diameter was decreased, the amount of minerals obtained from the underflow decreased and so the heavier minerals exited through the overflow. Bentonites are thus acquired that have smaller proportions of smectite and poorer swelling properties when smaller apex diameters were used. When the apex diameter was larger, bentonites with greater proportions of smectite and better swelling properties were obtained.

When the diameter of the vortex was increased, the amount of material in suspension was increased, meaning that more minerals exit *via* the overflow, thereby increasing the volume of solid suspension obtained from the overflow. The viscosity increased as a result and smectite enrichment was made more difficult. The amount of contaminator minerals obtained from the overflow increased and the smectite contents decreased as the vortex diameter was increased. A minimum diameter of the vortex and a maximum diameter of the apex are preferred in order to obtain optimal proportions of smectite and the best swelling properties.

Optimization of variables for the hydrocyclone for the three different bentonites

Optimization of the operational variables was achieved using quadratic programming of the mathematical software package *Minitab 15* (Minitab Inc., 2007) which gave the maximum proportion of smectite (%) and greatest degree of swelling (mL/2 g) for the Groups 1, 2, and 3 of bentonite (Table 9). Final tests were carried out to prove the accuracy of the results under optimum conditions; the results obtained (Tables 10, 11) were very close to the calculated results. The amounts of non-clay minerals such as cristobalite/Opal-CT, quartz, feldspar, calcite, and dolomite removed and the propor-

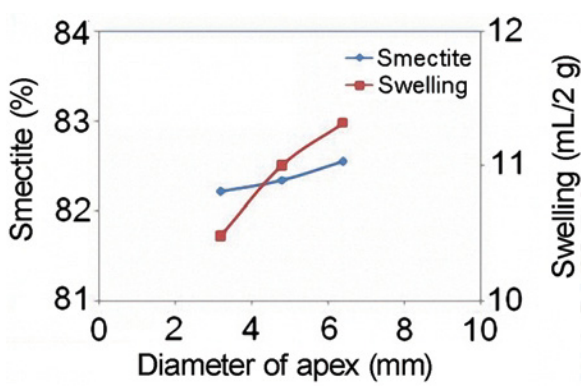

Figure 19. Variations of the smectite content and swelling with different vortex diameters for Group 1 bentonites at the mid-level of the other three variables.

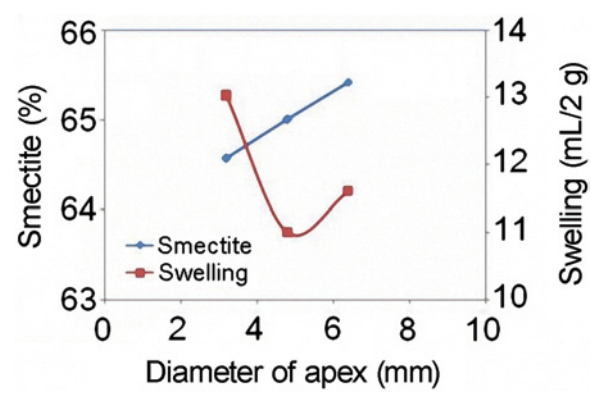

FIG. 21. Variations of the smectite content and swelling with different vortex diameters for Group 3 bentonites at the mid-level of the other three variables.

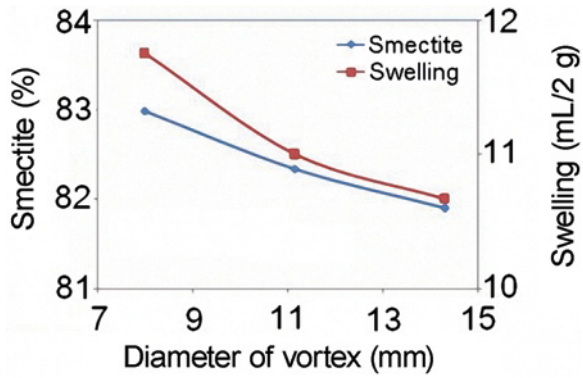

FIG. 22. Variations of the smectite content and swelling with different apex diameters for Group 1 bentonites at the mid-level of the other three variables.

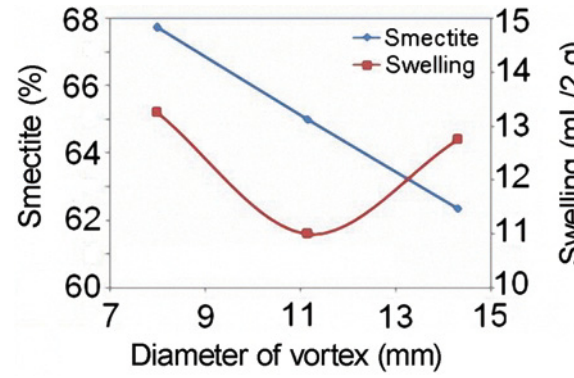

FIG. 24. Variations of the smectite content and swelling with different apex diameters for Group 3 bentonites at mid-level of the other three variables.

tion of smectite remaining increased in all three groups. The results of the chemical analyses support these results.

CONCLUSIONS

A three-level and Box–Behnken factorial design combined with a response surface methodology was employed for modeling and optimizing four operational variable parameters (feed solids (%), inlet pressure (bar), apex diameter (mm), and vortex diameter (mm)) of a hydrocyclone to produce bentonite concentrates. Three different bentonites in their natural states were investigated and found unsuitable for industrial use. The mathematical model equations were derived for both smectite content and swelling of bentonite concentrates by using sets of experimental data and the mathematical software package *Minitab 15* (Minitab Inc., 2007).

The predicted values match the experimental values reasonably well, with R^2 of 0.968 for smectite and R^2 of 0.829 for swelling of Group 1 bentonite concentrates. The corresponding values of R^2 for Group 2 were 0.973 for smectite and 0.991 for swelling, and 0.999 and 0.867 for Group 3, respectively.

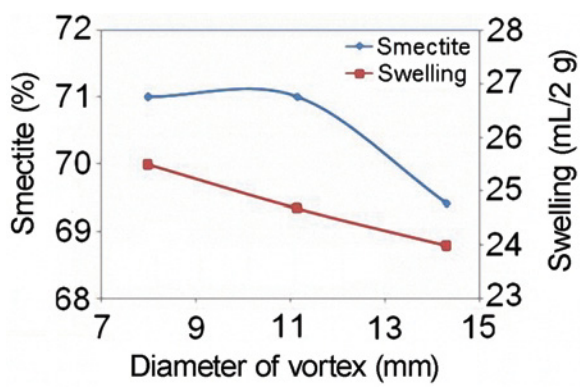

FIG. 23. Variations of the smectite content and swelling with different apex diameters for Group 2 bentonites at the mid-level of the other three variables.

As a result of the experimental studies, the proportion of smectite and the swelling values of all three bentonite groups increased substantially through hydrocyclone beneficiation. The greatest increase (81.45%) in the proportion of smectite was achieved for Group 3 bentonites. The greatest increase in swelling properties (194%) was obtained for Group 2 bentonites.

The proportion of smectite was increased by removing non-clay minerals such as feldspar, quartz, calcite, and dolomite and in this way the swelling capacity of the bentonites was also enhanced. In order to gain a better understanding of the effects of these operational variables of the hydrocyclone on the smectite content and swelling capacity of three groups of bentonite concentrates, the observed values were presented as a 2D matrix of smectite content and swelling capacity, with each variable calculated at the mid-level of the other three variables. The influence of the inlet pressure clearly varied in accordance with the proportion of smectite and with the particle-size fraction of the bentonites. As a result, a narrow vortex diameter and a broad apex diameter are preferred for processing with the hydrocyclone in order to acquire bentonite concentrate with the greatest proportion of smectite and the greatest swelling capacity. A large solid:liquid ratio cannot be used to beneficiate bentonites containing cristobalite and opal.

Using quadratic programming, a feed solids of 10%, an inlet pressure of 1.5 bar, an apex diameter of 6.4 mm, and a vortex diameter of 8 mm were determined as the optimum levels to achieve the largest proportion of smectite (84.84%) for Group 1 bentonite. For tests conducted, 84.0% was the value obtained, *i.e.* a 0.84% upgrading in the smectite could be obtained by quadratic programming. In the same way, a feed solids of 5%, inlet pressure of 2.5 bar, apex diameter of 6.4 mm, and vortex diameter of 8 mm were determined as optimum levels to achieve a swelling capacity of 13.92 mL/2 g for Group 1

Table 9. Optimization of variables of hydrocyclone on response (smectite and swelling).

Bentonites	Variables of hydrocyclone				Maximum predicted values obtained with variable of hydrocyclone	
	Feed solids (%)	Inlet pressure (bar)	Apex diameter (mm)	Vortex diameter (mm)	Smectite concentration (%)	Swelling (mL/2 g)
Group 1	10	1.5	6.4	8	84.84	13.42
	5	2.5	6.4	8	81.84	13.92
Group 2	10	2.5	6.4	8	93.08	29.42
Group 3	5	1.5	3.2	8	72.58	21.83
	5	1.5	6.4	8	68.25	22.62

Table 10. Mineralogical analysis of the bentonites obtained in the final experiments.

Group	Class	S	Ch	I	Cr/O	Q	F	Ca	D
1	Natural	54.00	1.00	1.00	2.00	3.00	40.00	2.00	0.00
	Beneficiation	84.00	12.00	0.00	0.00	0.00	3.00	1.00	1.00
2	Natural	55.00	0.00	0.00	5.00	2.00	32.00	3.00	3.00
	Beneficiation	93.00	0.00	0.00	0.00	0.00	7.00	0.00	0.00
3	Natural	40.00	0.00	2.00	7.00	4.00	30.00	9.00	8.00
	Beneficiation	73.00	0.00	0.00	2.00	0.00	13.00	0.00	5.00

S – Smectite, Ch – Chlorite, I – Illite, Cr/O – Cristobalite/Opal CT, Q – Quartz, F – Feldspar, Ca – Calcite and D – Dolomite.

bentonite, whereas it was 13.0 mL/2 g in the tests conducted, *i.e.* a 0.92 mL/2 g improvement could be obtained by programming. The same can be said for Group 2 and Group 3 bentonites. The present study demonstrates that the Box–Behnken design and the response surface methodology can be used successfully for modeling some of the operating parameters of a hydrocyclone used on the Sarıcakaya-Mihalgazi/Turkey bentonites. This approach also minimizes the time and number of experiments required to obtain the optimum hydrocyclone operating conditions to maximize performance. Results demonstrated that experimental observations closely matched those predicted by the method described here. This approach to beneficiation, which worked well at the laboratory scale, may apply also at the industrial scale, thus overcoming current limitations on the usefulness of Sarıcakaya-Mihalgazi/Turkey bentonites due to their low smectite content and swelling capacity.

Table 11. Chemical analysis (mass % of oxide) of bentonite obtained in the final experiments.

Component	Beneficiation of Group 1	Beneficiation of Group 2	Beneficiation of Group 3
Na_2O	1.48	1.68	1.66
MgO	2.88	4.12	5.03
Al_2O_3	21.43	17.85	14.15
SiO_2	54.67	55.92	57.22
P_2O_5	0.14	0.08	0.08
K_2O	0.40	2.03	1.87
CaO	1.48	0.66	2.34
MnO	0.06	0.02	0.03
TiO_2	0.55	0.63	0.68
Fe_2O_3	3.27	6.18	5.99
LOI	14.00	11.00	11.00
Total	100.36	100.17	100.05

LOI: loss on ignition

ACKNOWLEDGMENTS

The authors are grateful for funding from the Scientific and Technical Research Council of Turkey (TÜBİTAK), under Project # 104Y160.

REFERENCES

Adams, J.M. (1987) Synthetic organic chemistry using pillared cation exchanged and acid treated montmorillonite catalysis: a review. *Applied Clay Science*, **2**, 309–342.

Allo, W.A. and Murray, H.H. (2004) Mineralogy, chemistry and potential applications of a white bentonite in San Juan province. *Applied Clay Science*, **25**, 237–243.

Alther, G.R. (1986) The effect of the exchangeable cations on the physico-chemical properties of Wyoming bentonites. *Applied Clay Science*, **1**, 273–284.

Aslan, N. and Cebeci, Y. (2007) Application of Box–Behnken design and response surface methodology for modeling of some Turkish coals. *Fuel*, **86**, 90–97.

Aslan, N. (2007a) Application of response surface methodology and central composite rotatable design for modeling the

influence of some operating variables of a Multi-Gravity Separator for coal cleaning. *Fuel*, **86**, 769–776.

Aslan, N. (2007b). Modeling and optimization of Multi-Gravity Separator to produce celestite concentrate. *Powder Technology*, **174**, 127–133.

ASTM D 5890-95. Standard test method for swell index of clay mineral component of geosynthetic clay liners. *American Society for Testing and Materials.*

Barrer, R.M. (1989) Shape-selective sorbents based on clay minerals: a review. *Clays and Clay Minerals*, **37**, 385–395.

Biscaye, P.E. (1965) Mineralogy and sedimentation of recent deep sea clay in the Atlantic Ocean and adjacent seas and oceans. The Geological Society of America Bulletin, **76**, 803–832.

Box, G.E.P. and Behnken, D.W. (1960) Some new three level designs for the study of quantitative variables. *Technometrics*, **2**, 455–475.

Box, G.E.P. and Wilson, K.B. (1951) On the experimental attainment of optimum conditions. *Journal of the Royal Statistical Society*, **B13**, 1–45.

Box, G.E.P., Hunter, W.G., and Hunter, J.S. (1978) *Statistics for Experimenters: an Introduction to Design, Data Analysis, and Model Building*. John Wiley and Sons, New York, 653 pp.

Boylu, F., Çinku, K., Çetinel, T., Erkan, İ., and Demirer, N. (2007) The separation effeciency of Reşadiye Na-Bentonite by hyrdrocyclone. Pp. 12–14 in: *XIII. National Clay Symposium* (M. Kuşçu, O. Cengiz and E. Öener, editors), Isparta, Turkey.

Brown, G. (1972) Montmorillonites. Pp. 143–206 in: *X-ray Identification and Crystal Structures of Clay Minerals*. Mineralogical Society, London.

Brown, G. and Brindley, G.W. (1980) X-ray diffraction procedures for clay mineral identification. Pp 305-359 in: *Crystal Structures of Clay Minerals and their X-ray Identification* (G.W. Brindley and G. Brown, editors). Monograph **5**, Mineralogical Society, London.

Cebeci, Y. and Sönmez, I. (2006) Application of the Box–Wilson experimental design method for the spherical oil agglomeration of coal. *Fuel*, **85**, 289–297.

Christidis, G. and Scott, P.W. (1993) Laboratory evaluation of bentonites. *Industrial Minerals*, **311**, 51–57.

Christidis, G.E., Scott, P.W., and Dunham, A.C. (1997) Acid activation and bleaching capacity of bentonites from the islands of Milos and Chios Aegean, Greece. *Applied Clay Science*, **12**, 329–374.

Christidis, G. (1998) Physical and chemical properties of some bentonite deposits of Kimolos Island, Greece. *Applied Clay Science*, **13**, 79–98.

Chu, L.Y. and Luo, Q. (1994) Hydrocyclone with high sharpness of separation. *Filtration and Separation*, **31**, 733–736.

Chung, F. (1974) Quantitative interpretation of X-ray diffraction patterns of mixtures. I. Matrix flushing method for quantitative multicomponent analysis. *Journal of Applied Crystallography*, **7**, 519–525.

Correia, S.L., Curto, K.A.S., Hotza, D., and Segadães, A.M. (2004) Using statistical techniques to model the flexural strength of dried triaxial ceramic bodies. *Journal of the European Ceramic Society*, **24**, 2813–2818.

Ferreira, S.L.C., Dos Santos, W.N.L., Quintella, C.M., Neto, B.B., and Boque-Sendra, J.M. (2004) Doehlert matrix: a chemometric toll for analytical chemistry – review. *Talanta*, **63**, 1061–1067.

Ge, Z., Li, D., and Pinnavaia, T.J (1994) Preparation of alumina-pillared montmorillonite with high thermal stability, regular microporosity and Lewis/Brönsted acidity. *Microporous Materials*, **3**, 165–175.

Grim, R.E. (1962) *Applied Clay Mineralogy*. International Series in Earth Sciences. McGraw-Hill Book Company, New York, 421 pp.

Grim, R.E. (1968) *Clay Mineralogy*. McGraw-Hill Book Company, New York, 596 pp.

Grim, R.E. and Güven, N. (1978) *Bentonites: Geology, Mineralogy, Properties and Uses*. Developments in Sedimentology 24. Elsevier Publishing Company, New York, 256 pp.

Gunaraj, V. and Murugan, N. (1999) Application of response surface methodologies for predicting weld base quality in submerged arc welding of pipes. *Journal of Materials Processing Technology*, **88**, 266–275.

Gündoğdu, M.N. (1982) Geological, mineralogical and geochemical investigation of the Bigadiç Neogene volcano-sedimentary basin. Ph.D. thesis, Hacettepe University, Ankara, Turkey, 386 pp.

Güven, N. and Pollastro, R.M. (1992) *Clay–Water Interface and Its Rheological Implications, CMS Workshop Lectures*, vol. 4. The Clay Mineral Society, Aurora, CO, USA.

Habibian, M., Pazouki, M., Ghanaie, H., and Abbaspour-Sani, K. (2008) Application of hydrocyclone for removal of yeasts from alcohol fermentations broth. *Chemical Engineering Journal*, **138**(1–3), 30–34.

Hassan, M.S. and Abdel-Khalek, N.A. (1998) Beneficiation and applications of an Egyptian bentonite. *Applied Clay Science*, **13**, 99–115.

Johns, W.D., Grim, R.E., and Bradley, W.F. (1954) Quantitative estimations of clay minerals by diffraction methods. *Journal of Sedimentary Petrology*, **24**, 242–251.

Kahraman, S., Önal, M., Sarıkaya, Y., and Bozdoğan, İ. (2005) Characterization of silica polymorphs in kaolins by X-ray diffraction before and after phosphoric acid digestion and thermal treatment. *Analytica Chimica Acta*, **552**, 201–206.

Kincl, M., Turk, S., and Vrecer, F. (2005) Application of experimental design methodology in development and optimization of drug release method. *International Journal of Pharmaceutics*, **291**, 39–49.

Komadel, P., Bujdák, J., Madejová, J., Šucha, V., and Elsass, F. (1996) Effect of non-swelling layers on the dissolution of reduced-charge montmorillonite in hydrochloric acid. *Clay Minerals*, **31**, 333–345.

Komadel, P. (2003) Chemically modified smectites. *Clay Minerals*, **38**, 127–138.

Komine, H. and Ogata, N. (1994) Experimental study on swelling characteristics of compacted bentonite. *Canadian Geotechnical Journal*, **31**, 478–490.

Komine, H. and Ogata, S. (1996) Prediction for swelling characteristics of bentonite. *Canadian Geotechnical Journal*, **33**, 11–21.

Komine, H. and Ogata, S. (1999) Experimental study on swelling characteristics of sand-bentonite mixture for nuclear waste disposal. *Soils and Foundations*, **39**, 83–97.

Kwak, J.S. (2005) Application of Taguchi and response surface methodologies for geometric error in surface grinding process. *International Journal of Machine Tools and Manufacture*, **45**, 327–334.

Lagaly, G. (1984) Clay–organic interactions. *Philosophical Transactions of the Royal Society of London*, **A311**, 315–332.

Low, P.F. (1979) Nature and properties of water in montmorillonite–water systems. *Soil Science Society of America Journal*, **43**, 651–658.

Luckham, P.F. and Rossi, S. (1999) The colloidal and rheological properties of bentonite suspension. *Advances in Colloid and Interface Science*, **82**, 43–92.

Malfoy, C., Pantet, A., Monnet, P., and Righi, D. (2003) Effect of the nature of exchangeable cation and clay concentration on the rheological properties of smectite suspensions. *Clays and Clay Minerals*, **51**, 656–663.

Martinez, A.L., Uribe, A.S., Carrillo, F.R.P., Coreno, J.A., and Ortiz, J.C. (2003) Study of celestite flotation efficiency using sodium dodecyl sulfonate collector: factorial experiment and statistical analysis of data. *International Journal of Mineral Processing*, **70**, 83–97.

Massart, D.L., Vandeginste, B.G.M., Buydens, L.M.C., Jong, S., Lewi, P.J., and Smeyers Verbeke, J. (1997) *Handbook of Chemometrics and Qualimetrics Part A*. Elsevier Publishing Company, Amsterdam, 886 pp.

Minitab Inc. (2007) *Meet minitab 15.* USA, 142 pp.

Montes, G., Duplay, J., Martinez, L., Geraud, Y., and Rousset-Tournier, B. (2003) Influence of interlayer cations on the water sorption and swelling-shrinkage of MW80 bentonite. *Applied Clay Science*, **23**, 309–321.

Montgomery, D.C. (2001) *Design and Analysis of Experiments*, 5th edition. John Wiley & Sons, New York, 684 pp.

Murray, H.H. (2000) Traditional and new applications for kaolin, smectite and polygorskite: a general overview. *Applied Clay Science*, **17**, 207–221.

Neaman, A., Pelletier, M., and Villieras, F. (2003) The effects of exchangeable cation, compression, heating and hydration on textural properties of bulk bentonite and its corresponding purified montmorillonite. *Applied Clay Science*, **22**, 153–168.

Neto, B.B., Scarminio, I.S., and Bruns, R.E. (2001) *Como fazer Experimentos: Pesquisa e Desenvolvimento na Ciência e na Industria.* Editora da Unicamp, São Paulo, 480 pp.

Obeng, D.P., Morrell, S., and Napier-Munn, T.J. (2005) Application of central composite rotatable design to modeling the effect of some operating variables on the performance of the three-product cyclone. *International Journal of Mineral Processing*, **76**, 181–192.

Önal, M., Sarıkaya, Y., and Alemdaroğlu, T. (2002) The effect of acid activation on some physicochemical properties of a bentonite. *Turkish Journal of Chemistry*, **26**, 409–416.

Önal, M. (2007) Swelling and cation exchange capacity relationship for the samples obtained from a bentonite by acid activations and heat treatments. *Applied Clay Science*, **37**, 74–80.

Özbayoğlu, G. and Atalay, M.U. (2000) Beneficiation of bastnaesite by a multigravity separator. *Journal of Alloys and Compounds*, **303-304**, 520–523.

Özgen, S., Yıldız, A., Çalışkan, A., and Sabah, E. (2009) Modeling and optimization of hydrocyclone processing of low grade bentonites. *Applied Clay Science*, **46**, 305–316.

Pinnavaia, T.J. (1983) Intercalated clay catalysis. *Science*, **220**, 365–371.

Push, R. (1992) Use of bentonite for isolation of radioactive waste products. *Clay Minerals*, **27**, 753–761.

Ragonese, R., Macka, M., Hughes, J., and Petocz, P. (2002) The use of the Box-Behnken experimental design in the optimisation and robustness testing of a capillary electrophoresis method for the analysis of ethambutol hydrochloride in a pharmaceutical formulation. *Journal of Pharmaceutical and Biomedical Analysis*, **27**, 995–1007.

Rickwood, D., Onions, J., Bendixen, B., and Smyth, I. (1992) Prospects for the use of hydrocyclones for biological separations. Pp. 109–120 in: *Hydrocyclones Analysis and Applications* (L. Svaorovsky and M.T. Thew, editors). Kluwer Academic, London.

Rytwo, G., Serben, C., Nir, S., and Margulies, L. (1991) Use of methylene blue and crystal violet for determination of exchangeable cations in montmorillonite. *Clays and Clay Minerals*, **39**, 551–555.

Sarıkaya, Y., Önal, M., Baran, B., and Alemdaroğlu, T. (2000) The effect of thermal treatment on some of the physicochemical properties of a bentonite. *Clays and Clay Minerals*, **48**, 557–562.

Sharmm, L.L. and Kwak, J.C.T. (1982) Influence of exchangeable cation composition on the size and shape of montmorillonite particles in dilute suspension. *Clays and Clay Minerals*, **30**, 40–48.

Souzaa, A.S., dos Santos, W.N.L., and Sergio Ferreira, L.C. (2005) Application of Box–Behnken design in the optimization of an on-line pre-concentration system using knotted reactor for cadmium determination by flame atomic absorption spectrometry. *Spectrochimica Acta Part B*, **60**, 737–742.

Tan, Ö., Yılmaz, L., and Zaimoğlu, S. (2004) Variation of some engineering properties of clays with heat treatment. *Materials Letters*, **58**, 1176–1179.

Theng, B.K.G. (1974) *The Chemistry of Clay Organic Reactions*. Adam Hilger, London.

Wersin, P., Curti, E., and Appelo, C.A.J. (2004) Modeling bentonite–water interactions at high solid/liquid ratios: swelling and diffuse double layer effects. *Applied Clay Science*, **26**, 249–257.

Williams, R.A., Albarran de Garcia Colon, I.L., Lee, M.S., and Roldan Villasana, E.J. (1994) Design Targeting of Hydrocyclone Networks. *Minerals Engineering*, **7**, 561–576.

Xiao, Z. and Vien, A. (2004) Experimental designs for precise parameter estimation for non-linear models. *Minerals Engineering*, **17**, 431–436.

Varma, R.S. (2002) Clay and clay-supported reagents in organic synthesis. *Tetrahedron*, **58**, 1235–1255.

Yıldız, A., Kibici, Y., Çoban, F., Bağcı, M., Dumlupunar, İ., Kocabaş, C., Arıtan, E., and Bilge Y. (2008) *The investigation of the geological properties of Mihalgazi (Eski*şehir) bentonite and evaluation of bentonite as industrial raw material. The Scientific and Technical Research Council of Turkey (TÜBİTAK) Project No: 104Y160 Technical Report, Turkey.

Yıldız, A. and Kuşcu, M. (2007) Mineralogy, chemistry and physical properties of bentonites from Başören, Kütahya, W-Anatolia. *Clay Minerals*, **42**, 403–418.

Yong, R.N. (1999) Soil suction and soil–water potential in swelling clays in engineered clay barriers. *Engineering Geology*, **54**, 3–13.

(*Received 24 September 2008; revised 6 February 2010; Ms. 201; A.E. R.W. Brown*)